Journal of Sedimentary Research

Journal of Sedimentary Research, 2016, v. 86, 59–72
Research Article
DOI: http://dx.doi.org/10.2110/jsr.2016.1

NANO-CRYSTAL FORMATION OF TIO_2 POLYMORPHS BROOKITE AND ANATASE DUE TO ORGANIC–INORGANIC ROCK–FLUID INTERACTIONS

HANS-MARTIN SCHULZ,[1] RICHARD WIRTH,[2] AND ANJA SCHREIBER[3]

[1]*Helmholtz Centre Potsdam–GFZ German Research Centre for Geosciences, Section 3.2 Organic Geochemistry, Telegrafenberg, D-14473 Potsdam, Germany*
[2]*Helmholtz Centre Potsdam–GFZ German Research Centre for Geosciences, Section 4.3 Chemistry and Physics of Earth Materials, Telegrafenberg, D-14473 Potsdam, Germany*
[3]*Helmholtz Centre Potsdam–GFZ German Research Centre for Geosciences, Section 4.2 Geomechanics and Rheology, Telegrafenberg, D-14473 Potsdam, Germany*
e-mail: schulzhm@gfz-potsdam.de

ABSTRACT: **The occurrence of the titania polymorphs brookite and anatase as nano-crystals in organic matter-rich sediments of differing age and thermal maturity has been investigated by means of a multidisciplinary analytical approach (FIB-TEM, organic geochemistry, and petrography). It was the aim of the study to analyze the formation mechanisms, fate and behavior of the titania nano-crystals as a result of organic–inorganic rock–fluid interactions.**

Brookite nano-crystals have been detected in immature Mediterranean sapropels of Quaternary age, but anatase also occurs in deeper and older black shales (Furongian Alum Shale, Sweden; Devonian to Carboniferous Bakken Shale, Williston Basin, USA). Whereas anatase prevails as single crystals, brookite nano-crystals often are agglomerated. Single brookite nano-crystals from Posidonia Shale (Lower Jurassic, Northern Germany) have increasing crystal diameters with increasing thermal maturity.

Exclusively anatase nano-crystals both as single crystals or as agglomerates have been detected at oil–water contacts in oilfields, and along fractures with fluid flow enriched in dissolved organic carbon.

Titania nano-crystal precipitation, growth (and agglomeration) takes place in the pore water of micro-environments at low to high temperatures and where low pH is coupled to the occurrence of dissolved organic components. Low sedimentation rates preserving a critical geochemical environment or higher temperatures seem major controls for the precipitation of anatase and its tendency not to agglomerate.

INTRODUCTION

In nature titania (TiO_2) occurs mainly in the form of three polymorphs: thermodynamically most stable rutile, anatase (both tetragonal), and orthorhombic brookite. Anatase and brookite are metastable, occur at low temperatures and pressures, and may directly transform to rutile without involvement of the other metastable phase (Huberty and Xu 2008). However, the reasons for the formation of the metastable polymorphs anatase and brookite in nature instead of rutile are poorly understood, especially at low temperatures (Post and Burnham 1986). One controlling factor may be the different enthalpy of the three TiO_2 polymorphs which is dependent on the specific surface area (Ranade et al. 2002). The influence of organic matter and its degradation products may be another factor.

In sedimentary basins TiO_2 nanoparticles are described from black shales which are typically rich in organic carbon (e.g., Bernard et al. 2012; Tuschel 2013). Black shales already undergo complex diagenetic processes during deposition of organic-rich mud at the sediment–water interface. Such processes take place as interactions between solids, gas phases, and fluids, and the involved phases can be inorganic or organic in nature. Such interactions are widespread in sedimentary basins and also occur at great burial depth. In general, these complex geochemical processes take place in aqueous solutions in which pH may be a major control for the phase stability of titania nanoparticles. Very low pH, e.g., stabilizes small rutile against anatase, but greater stability of rutile crystal size is independent of pH (Finnegan et al. 2007). The irreversible conversion (or mineralization) of organic carbon—in a more general sense "organic matter"—is the driving force for such complex interrelated processes in sediments. The conversion of labile organic compounds leads to significant geochemical changes of the pore fluid such as pH, alkalinity, etc., which may control the formation of, e.g., nanometer-size diagenetic titania. Many such organic–inorganic interactions are known from petroleum-bearing sedimentary basins (Helgeson et al. 1993; Seewald 2003; van Berk et al. 2013). Not directly transferable in this context, but comparable to sedimentary pore fluids are wastewaters. Environmental studies about the behavior of titania nanoparticles in the presence of wastewater-derived organic matter indicate that TiO_2 nanoparticles strongly settle out of solution, in contrast with their behavior in solutions with humic acids (Neale et al. 2015). In contrast, the mean TiO_2 nanoparticle diameter increases in wastewater whereas it remains nearly constant in humic acid.

To date, only a few investigations have focused on diagenetic TiO_2 nanoparticles to unravel organic–inorganic interactions which may control brookite or anatase precipitation in sediments. The study of such interactions during titania formation requires the development of new paradigms to understand how these complex systems function. Up to now, the transition from anatase to rutile has mostly been studied intensely (Banfield et al. 1993), but brookite formation and the controlling factors in sedimentary environments are unknown. The phase stability field of brookite thus remains undefined. This is due to the fact that reaction conditions that lead to the selective growth and nucleation of brookite are more restrictive, because of a small stability window compared to those required to form anatase or rutile. Moreover, the diagnostic procedures

Published Online: February 2016
 1527-1404/16/086-59/$03.00

TABLE 1.—*Origin of the investigation material.*

Sample No.	Name	Stratigraphy	Location	Well Depth (m)
G014094	Mediterranean Sapropel S1	Holocene	Eastern Mediterranean Sea	0.27 m, at 3,090 m water depth
G014095	Mediterranean Sapropel S5	Pleistocene	Eastern Mediterranean Sea	2.70 m, at 2,788 m water depth
G014096	Mediterranean Sapropel S6	Pleistocene	Eastern Mediterranean Sea	4.12 m, at 2,788 m water depth
G011700	Alum Shale	Furongian (Upper Cambrian)	Southern Sweden	74.42
G011702	Alum Shale	Furongian (Upper Cambrian)	Southern Sweden	75.45
G011703	Alum Shale	Furongian (Upper Cambrian)	Southern Sweden	77.35
-	Schöneck Fm.	Oligocene	Upper Austria	1,384
G005270	Bakken Shale	Upper Devonian–Lower Mississippian	Williston Basin (North Dakota, USA)	2,332
G005277	Bakken Shale	Upper Devonian–Lower Mississippian	Williston Basin (North Dakota, USA)	2,344
G005298	Bakken Shale	Upper Devonian–Lower Mississippian	Williston Basin (North Dakota, USA)	1,010
G007143	Posidonia Shale	Toarcian (Liassic)	Lower Saxony (Germany)	45.7
G007049	Posidonia Shale	Toarcian (Liassic)	Lower Saxony (Germany)	55.7
G007098	Posidonia Shale	Toarcian (Liassic)	Lower Saxony (Germany)	46.1
#2953	Wealden	Earliest Cretaceous	Lower Saxony (Germany)	926
#1856	SAFOD	?	USA	3,194
G012222	Heimdal Fm.	Miocene	Oil–water contact in sandstone, Danish North Sea	2,116, at 58 m water depth

to clearly identify brookite phases on a nanometer scale are often complex, needing high-resolution imaging techniques (such as transmission electron microscopy, TEM) and identification procedures, and, at least, are often not in the focus of research projects.

In this manuscript we aim to answer the following questions:

- How does organic diagenesis or diagenetic products such as CO_2, CH_4, H_2, or low-molecular-weight organic acids (LMWOAs) control the formation of nanometer-size brookite or anatase?
- Is brookite and anatase formation restricted to a specific content of total organic carbon (TOC) in TOC-rich sediments? If so, do these titania nanocrystals continue to grow during burial in a sedimentary basin?
- What geochemical conditions are needed for brookite or anatase precipitation, and what role does aggregation play in sediments?
- Is brookite or anatase formation restricted to immature black shales, or does it also take place in other sedimentary environments rich in organic carbon such as in oil fields?

To start answering these questions, firstly we summarize what is known about organic–inorganic interactions in sediments which may lead to brookite or anatase formation. In this section, we make a brief digression into the procedures used today in industrial production of anatase and brookite, and summarize which physicochemical frame is required which may relate to geochemical processes. Then we report our results from investigations of fine-grained sediments of differing ages, TOC contents, and thermal maturity in terms of organic diagenesis. Moreover our results include data from investigations

TABLE 2.—*Thermal maturity (vitrinite reflectance, R_r), organic-matter type and Rock Eval data (HI, OI, Tmax), and TiO_2 polymorph type of the investigation material. Origin of data: (i) Mediterranean sapropels: J. Möbius (Hamburg; personal communication); (ii) Alum Shale (Schulz et al. 2015); (iii) Schöneck Formation (Schulz et al. 2002); (iv) Bakken Shale (Kuhn et al. 2010); (v) Posidonia Shale (Bernard et al. 2012); (vi) Wealden (Lüders, personal communication); (vii) SAFOD (Janssen et al. 2014); (viii) Heimdal Formation (Mu et al. 2015).*

Sample No.	Name	R_r (%)	Total Organic Carbon (TOC, wt.%)	Organic-Matter Type	Hydrogen Index HI (mg HC/g TOC)	Oxygen Index OI (mg CO_2/g TOC)	Tmax (°C)	TiO_2 Polymorph
G014094	Mediterranean Sapropel S1	~ 0.3	1.5–2.0	marine	n.d.	n.d.	n.d.	**Brookite**
G014095	Mediterranean Sapropel S5	~ 0.3	7.1–8.5	marine	n.d.	n.d.	n.d.	**Brookite**
G014096	Mediterranean Sapropel S6	~ 0.3	4.0–5.5	marine	n.d.	n.d.	n.d.	**Brookite**
G011700	Alum Shale	0.42	14.3	marine	518	2	424	*Anatase*
G011702	Alum Shale	0.42	n.d.	marine	n.d.	n.d.	n.d.	**Brookite**
G011703	Alum Shale	0.42	n.d.	marine	n.d.	n.d.	n.d.	*Anatase*
-	Schöneck Fm.	0.4	3.6	lacustrine	550	n.d.	430	**Brookite**
G005270	Bakken Shale	0.5	16.35	marine	468	7	427	**Brookite**
G005277	Bakken Shale	0.5	8.48	marine	221	15	427	**Brookite** + *Anatase*
G005298	Bakken Shale	0.4	8.25	marine	416	27	413	**Brookite**
G007143	Posidonia Shale	0.53	10.8	marine	617	15	430	**Brookite**
G007049	Posidonia Shale	0.88	11	marine	282	5	449	**Brookite**
G007098	Posidonia Shale	1.45	6.77	marine	83	7	468	**Brookite**
#2953	Wealden	1.6	3.3	terrestrial	29	16	532	*Anatase*
#1856	SAFOD	n.d.	n.d.	-	n.d.	n.d.	n.d.	*Anatase*
G012222	Heimdal Fm.	n.d.	n.d.	oil–water contact	n.d.	n.d.	n.d.	*Anatase*

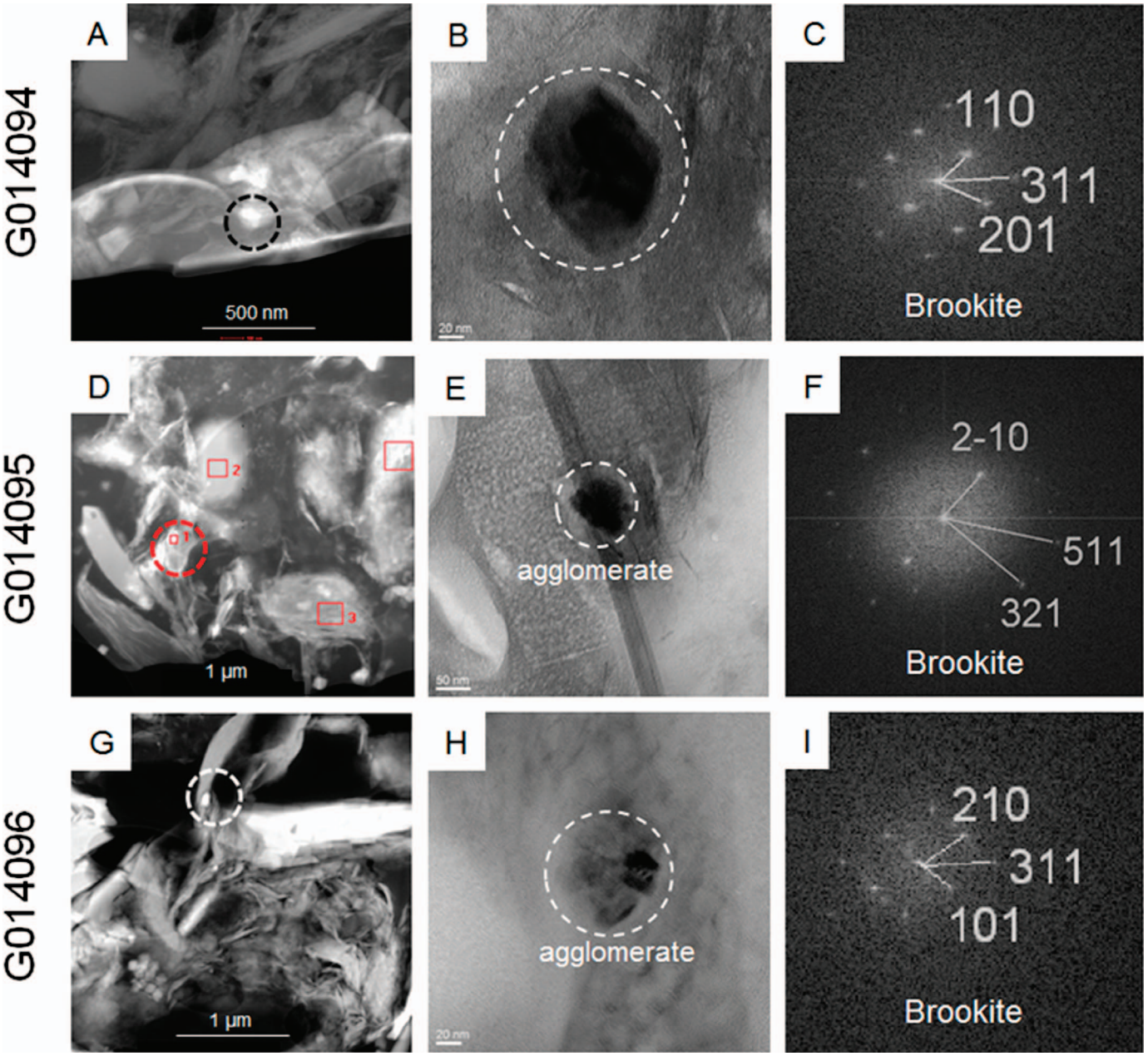

FIG. 1.—Mediterranean sapropels (see Tables 1–3 for sample characteristics). **A**, **D**, **G)** High-magnification scanning transmission electron microscopy (STEM) images (high-angle annular dark-field (HAADF) mode) showing brookite crystals (dotted circles). **B**, **E**, **H)** TEM Bright Field images of brookite crystals. Brookite occurs either as single crystals (B) or in the form of agglomerates (E, H). **C**, **F**, **I)** FFT diffraction pattern of crystals shown in Parts B, E, and H proving that brookite is the titania polymorph. Numbers in Parts C, F, and I indicate indices of imaging vectors. Note that the brookite crystal in Part B is a magnification of Part A. Labelled boxes are from point analyses to identify TiO_2 crystals.

about brookite formation in an oil-filled reservoir sandstone and along fractures with fluid flow.

Brookite and anatase from the TiO_2 system are ideal for studies of polymorphic phase transformations because both often (co-)occur in many fine-grained sediments. Especially fine-grained sediments may have a high TOC content, and the products of organic matter degradation may trigger titania precipitation, but also have primary Ti-bearing minerals which may serve as sources for Ti release during diagenesis.

In the laboratory the synthesis of nanobrookite can be governed by standardized laboratory conditions. It is thus important to note that the interpretation of factors which might have controlled the formation of titania nano-crystals in sedimentary basins is limited because geological systems are complex and have changed over time in terms of hydrogeochemical composition and many other parameters.

TITANIA FORMATION DUE TO ORGANIC–INORGANIC INTERACTIONS IN SEDIMENTS: A BRIEF REVIEW

Titanium is generally low in mobility unless hydrogeochemical conditions below pH 2 (a value of pH < 4.5 is given by other authors) are reached (Brookins 1988). However, titanium is mobilized in the presence of organic acids, which can form chelation complexes with Ti^{4+}. In natural water titanium exists only in a fully hydrated form. Such $TiO(OH)_2$ may occur in water with pH > 2, and such hydrates can be transported in colloidal state rather than as dissolved

TABLE 3.—*Indices of titania polymorphs and agglomeration in black shale.*

Sample No.	Name	R_r (%)	Angle	Calculated Angle (°)	Observed Angle (°)	TiO_2 Polymorph	Agglomerate (Yes/No)
G014094	Med.Sapropel S1	~ 0.3	∠110/311	39.6	39.76	**Brookite**	n
			∠201/311	28	27.85		
G014095	Med. Sapropel S5	~ 0.3	∠511/321	27.98	27.53	**Brookite**	y
			∠511/2$\bar{1}$0	60.52	61.76		
G014096	Med. Sapropel S6	~ 0.3	∠311/201	29.32	28.9	**Brookite**	**y**
			∠311/101	38.70	41.0		
			∠210/11$\bar{1}$	45.75	46.7	**Brookite**	**y**
			∠$\bar{1}$0$\bar{1}$/11$\bar{1}$	66.21	64.0		
G011700	Alum Shale	0.42	∠013/011	28.35	31.70	*Anatase*	n
			∠013/002	39.95	46.55		
G011702	Alum Shale	0.42	∠310/111	50.2	49	**Brookite**	y
			∠310/20$\bar{1}$	49.4	49		
G011703	Alum Shale	0.42	∠123/121	18.01	18.1	*Anatase*	n
			∠123/002	61.90	62		
-	Schöneck Fm.	0.4	∠112/210	63	63.3	**Brookite**	y
			∠112/$\bar{1}$02	38.91	38.3		
			∠002/$\bar{1}\bar{1}$1	47.64	48.3	**Brookite**	y
			∠002/111	47.64	48.3		
G005270	Bakken Shale	0.5	∠201/1$\bar{1}$0	67.01	71.0	**Brookite**	y
			∠201/111	43.10	43.0		
			∠0$\bar{2}$1/1$\bar{1}$0	40.57	40.0	**Brookite**	y
			∠0$\bar{2}$1/$\bar{1}\bar{1}\bar{1}$	28.70	27.9		
G005277	Bakken Shale	0.5	∠311/201	27.85	28.3	**Brookite**	n
			∠311/110	39.76	39.4		
			∠105/011	70.71	69	*Anatase*	n
			∠105/1$\bar{1}$4	28.50	28.3		
G005298	Bakken Shale	0.4	∠111/$\bar{1}$01	66.21	68.8	**Brookite**	n
			∠111/210	45.75	43.25		
			∠131/210	42.5	40.5	**Brookite**	n
			∠131/$\bar{1}$21	26.6	26		
			∠$\bar{1}$21/$\bar{3}$11	39.07	39.64	**Brookite**	n
			∠$\bar{3}$11/$\bar{2}\bar{1}$0	71.80	72.40		
G007143	Posidonia Shale	0.53	∠221/210	30.76	31.0	**Brookite**	n
			∠111/011	33.02	33.7		
G007049	Posidonia Shale	0.88	∠120/011	48.88	46.8	**Brookite**	n
			∠120/11$\bar{1}$	44.28	45		
G007098	Posidonia Shale	1.45	∠1$\bar{2}$0/1$\bar{1}$1	59.89	60.1	**Brookite**	n
			∠$\bar{1}\bar{2}$0/$\bar{2}\bar{1}\bar{1}$	46.40	45.35		
			∠102/$\bar{1}$01	44.9	44.8	**Brookite**	n
			∠102/210	32.6	33.3		

ions (Skrabal 1995). In contrast, concentrations of purely dissolved Ti^{4+} ions generally decrease with increasing contents of total dissolved solids. However, higher Ti^{4+} concentrations in organic-rich water provide further evidence of colloidal transport. Titanium may be removed from water by flocculation of colloidal material, and by adsorption and scavenging by precipitation of Mn and Fe oxides (Skrabal 1995).

Aggregation of titania nanoparticles in natural waters has been intensively studied. Today it is general consensus that, independent of pH, an increase in ionic strength generally results in increased aggregation, but also in higher adsorption of natural organic matter (Chen et al. 2012). In contrast, higher adsorption of natural organic matter, e.g., fluvial fulvic acids, leads to less aggregation of TiO_2 nanoparticles (Domingos et al. 2009; Keller et al. 2010). However, the adsorption intensity of humic acids on anatase nanoparticles is strongly dependent of pH of aqueous solutions. Yang et al. (2009) showed that the adsorption of humic acids strongly increases below a pH value of 5 to 6 as well as the zeta potential, and that this prevents aggregation. Furthermore, results of generic experiments in aqueous solution independent on pH showed that the smaller the titania nanoparticles the larger the aggregates. Addition of oxalic acid, a typical product of early diagenesis in TOC-rich sediments, promotes aggregation, and aggregation is higher at pH 6.5 than at pH 2 (Pettibone et al. 2008).

In contrast to the commonly held view of titanium immobility, there is abundant evidence for dissolution of titanium-bearing phases in siliciclastic sedimentary rocks, followed by the mobility and precipitation of authigenic titania (Morad 1986; Morad and Aldahan 1986, 1987a, 1987b). The role of water and dissolved organic compounds in the dissolution, transport, and precipitation of titania has been studied within the scope of soil studies (Swaine and Mitchell 1960; Fitzpatrick et al. 1978; Dumon and Vigneau 1979) and demonstrated that anatase and rutile can be dissolved by organic acids such as acetic acid and oxalic acid. In 1999, Cornu and co-authors reported that the Ti-bearing minerals rutile and anatase are not resistant against weathering in Amazonian ferralsol at a pH value of 4.5, and that there is reprecipitation of anatase. The authors concluded that Ti mobility may be linked to the complexing capacity of the organic compounds found in the soil solution. In general, dissolved titanium is regarded to rapidly precipitate as a hydrous oxide and subsequently to crystallize to anatase and rutile in soils (Fitzpatrick and Chittleborough 2002). Important to the presented results is that Ti gel-like phases in soil kaolinite particles may indicate Ti mobility at a grain scale

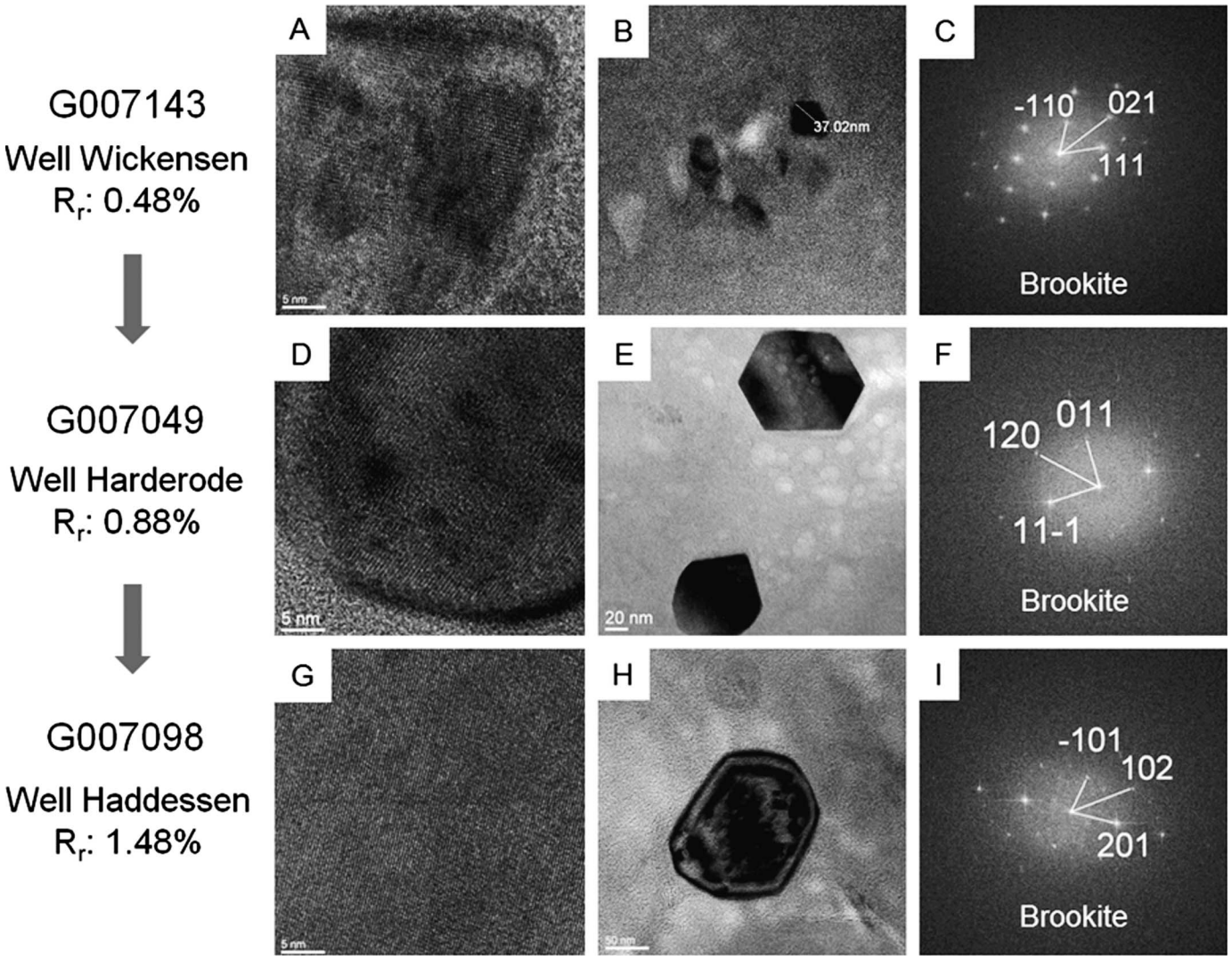

FIG. 2.—Posidonia Shale of differing thermal maturity (see vitrinite reflectance data on the right, and Tables 1–3 for sample characteristics). **A**, **D**, **G)** High-magnification scanning transmission electron microscopy (STEM) images (high-angle annular dark-field (HAADF) mode) showing brookite crystals. **B**, **E**, **H)** TEM Bright Field images of brookite single crystals. **C**, **F**, **I)** FFT diffraction patterns of crystals shown in Parts B, E, H proving that brookite is the titania polymorph. Zone axis in 2i is [010].

(Malengreau et al. 1995). Moreover, the hydrogeochemical system and the involved processes in soil (e.g., Schroeder and Shiflet 2000; Fang et al. 2009) can suggest a process analogue for organic–inorganic interactions during diagenesis in deeper TOC-bearing sediments (cf. Deng and Dixon 2002).

The first process studies about organic–inorganic interactions during diagenesis and the control of pore-water composition on formation of authigenic brookite and anatase were published by Hays et al. (1994). The authors interpreted diagenetic titania precipitates as the result of complexing of titanium by organic ligands. In this scenario, organic acids were regarded as mobilization agents followed by subsequent precipitation due to the decay of organo-titanium complexes. Furthermore, dissolved organic compounds may control the transport and precipitation of titania at higher temperatures, e.g., by hydrocarbon-rich fluids percolating through organic-rich shales (Parnell 2004). At lower temperatures, anatase nanoparticles may also form after dissolution by organic ligands in ground water and follow sol–gel-like processes leading to precipitation (Cabral et al. 2012). Complexation may thus explain titanium mobility at varying temperatures. A potential complexation candidate is ortho-titanic acid, which forms under acidic conditions in modern soils (Fitzpatrick et al. 1978), but complexes of titanium with carbonate ions or organic ligands are also considered (Hays et al. 1994). Additionally, the co-occurrence of diagenetic titania with either authigenic fluorapatite or crandallite may indicate that titania solubility is enhanced by phosphate complexation (Pe-Piper et al. 2011).

Rather special settings to study formation of titania nano-crystals are oilfields in which formation water and oil at elevated temperatures and pressures coexist at oil–water contacts (OWC). However, titanium occurs at low concentrations in oilfield waters (ppb; Collins 1975), and very close sources have to be considered.

Today, technical sol–gel processes to produce titania nanomaterials at low temperatures are carried out under controlled physicochemical conditions. Several parameters may serve as important key factors for comparison with subsurface conditions to find similar controls on formation of brookite and anatase, and fate and behavior in organic-rich sediments or environments. The most important chemical parameter in aqueous sol–gel experiments to produce nano-crystals of brookite or anatase is low pH. Further controls to prevent agglomeration of nano-crystals are low ionic strength and high contents of

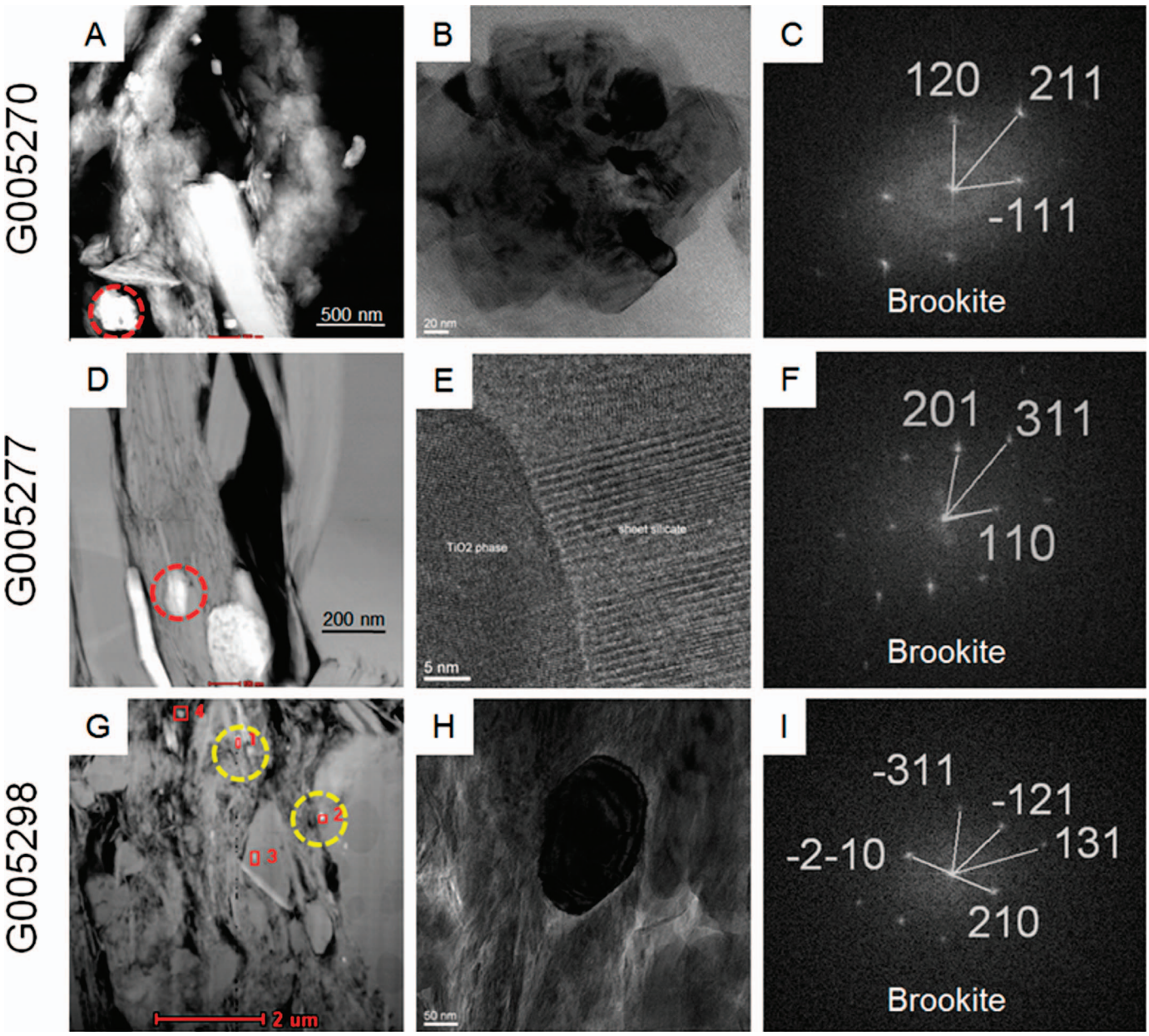

FIG. 3.—Bakken Shale (see Tables 1–3 for sample characteristics). **A**, **D**, **G)** High-magnification scanning transmission electron microscopy (STEM) images (high-angle annular dark-field (HAADF) mode) showing brookite crystals (dotted circles). **B**, **E**, **H)** TEM Bright Field images of brookite single crystals. **C**, **F**, **I)** FFT diffraction pattern of crystals shown in Parts B, E, H proving that brookite is the titania polymorph. Zone axis in 3c is [2-13].

acetic acid (and others, e.g., oxalic acid, fulvic and humic acid). For details see Bhave and Lee (2007), French et al. (2009), Isley and Penn (2006, 2008), and Isley et al. (2006, 2009).

CONCEPTUAL APPROACH

Sample Selection

TOC-rich fine-grained sediment samples of various thermal maturities and stratigraphic levels (Tables 1, 2) have been selected to investigate at which diagenetic stages brookite or anatase form in the presence of reactive and soluble (and thus convertible) organic material, and how such diagenetically formed titania changes during further diagenesis. In terms of stratigraphy the samples range from Furongian (Alum Shale) to Quaternary age (Mediterranean sapropels). The thermal maturity of the investigated samples ranges from immature conditions (Mediterranean sapropels) up to gas-window maturity (Toarcian Posidonia Shale, northern Germany, Hils half-graben). The samples of Posidonia Shale have different thermal maturities, ranging from pre-(early) oil conditions (R_r: 0.53%) over oil maturity (R_r: 0.88%) to the beginning of dry gas formation (R_r: 1.45%), and thus represent a natural maturation sequence.

Besides this basic sample set and the basic considerations that brookite (or anatase) forms in TOC-rich, thermally immature black shale, additional samples were selected to investigate whether titania also forms when convertible and soluble oil or gas phases are present. For this, one Wealden black shale sample (lacustrine to fluvial facies of Early Cretaceous sediments in northern Germany) and two sandstone samples from the oil–water contact (OWC) in

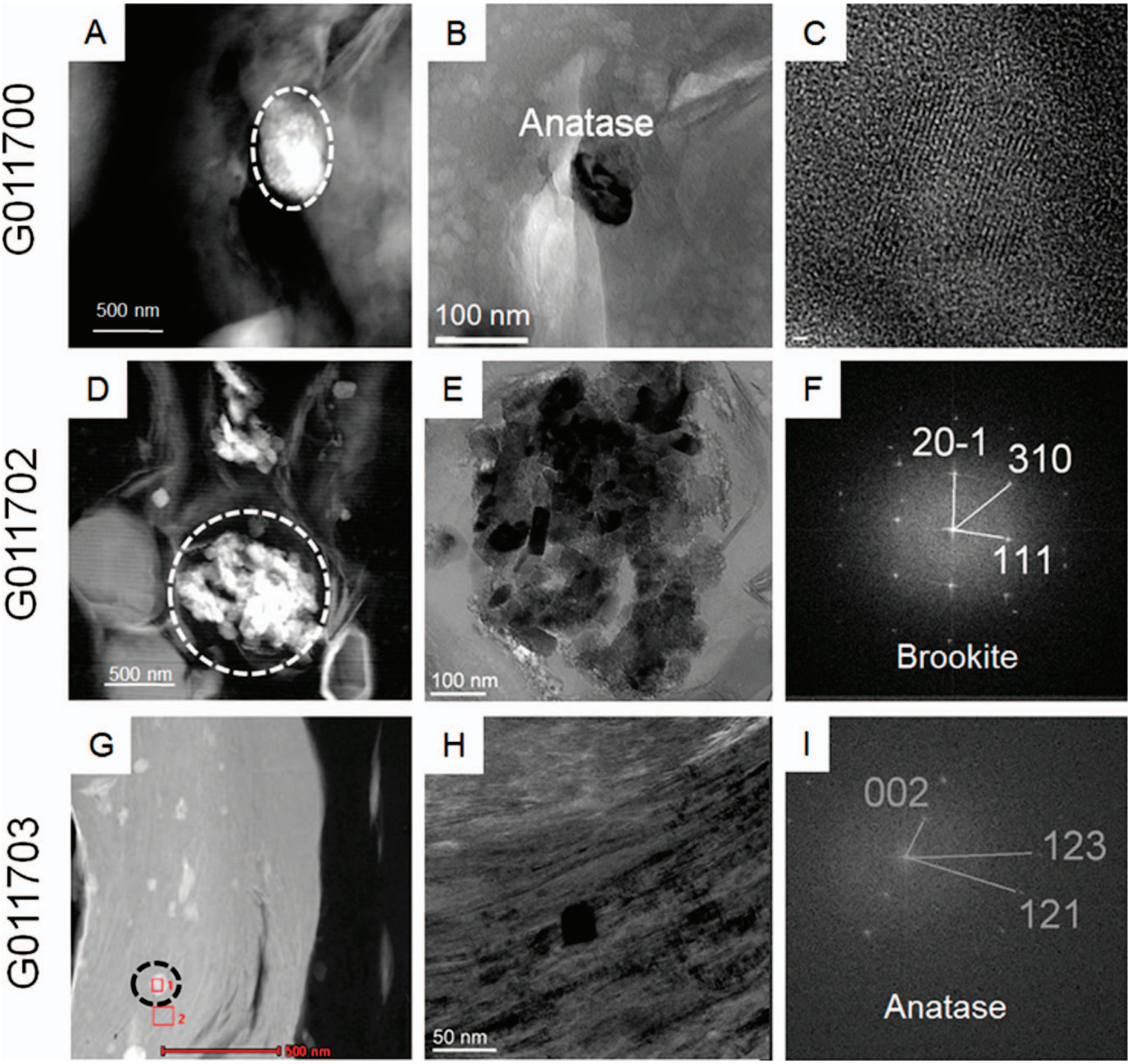

FIG. 4.—Alum Shale (see Tables 1–3 for sample characteristics). **A**, **D**, **G)** High-magnification scanning transmission electron microscopy (STEM) images (high-angle annular dark-field (HAADF) mode) showing brookite and anatase crystals (dotted circles). **B**, **E**, **H)** TEM Bright Field images of an agglomerate of brookite crystals (E) and of anatase single crystals (B, H). **F**, **I)** FFT diffraction pattern of crystals shown in Parts E, H proving that brookite and anatase are the titania polymorphs. **C)** HREM image of anatase.

the Siri field in the Danish North Sea (reservoir: glauconite-bearing sandstone of the Paleocene Heimdal Formation) were selected. Additionally, two shaly samples from the SAFOD (San Andreas Fault Observatory at Depth) well have been taken to investigate brookite formation along a fault with aqueous fluid flow containing hydrocarbons (Tables 1, 2).

The selected Wealden sample is from an altered flank of a graben structure in the Lower Saxony basin where hot basinal brines circulated and an unusually high degree of maturation was caused in contrast to the surrounding sediments.

The two samples from the Siri field (one from the oil leg, and one from the oil–water contact, OWC) have undergone severe diagenetic changes (e.g., berthierine formation as a consequence of glauconite dissolution, etc.; Mu et al. 2015) as both the oil leg and the OWC are reactive interfaces where soluble hydrocarbons are converted into carbon dioxide, methane, and acetic acid.

The investigated sample from the SAFOD well G is the "2" sample from a depth of 3,194 m (Janssen et al. 2014) where temperatures of 110–115°C prevail (Lockner et al. 2011) and where methane-rich fluids occur (Erzinger et al. 2006).

Besides geological age and well depth, basic organic geochemical data are available for selected samples. These are total organic carbon (TOC) content, vitrinite reflectance (R_r %), organic-matter type, and Rock Eval data (hydrogen index HI, oxygen index OI, and Tmax; Table 2).

TABLE 4.—*Indices of titania polymorphs and agglomeration in samples others than black shale.*

Sample No.	Name	R_r (%)	Angle	Calculated Angle (°)	Observed Angle (°)	TiO_2 Polymorph	Agglomerate (Yes/No)
#2953	Wealden	1.6	∠204/213	24.41	25.3	*Anatase*	*n*
			∠204/01/$\bar{1}$01/	76.69	76.6		
			∠$\bar{2}\bar{2}\bar{2}$/0$\bar{1}$1	57.84	57.6		
			∠$\bar{2}\bar{2}\bar{2}$/$\bar{2}\bar{1}\bar{3}$	21.07	20.95		
#1856	SAFOD	n.d.	∠112/011	41.07	41.64	*Anatase*	*y*
			∠112/101	41.07	40.94		
G012222	Heimdal Fm.	n.d.	∠013/011	28.35	28.3	*Anatase*	y + n
			∠013/002	39.95	40.5		
			∠022/013	28.33	29		
			∠022/01$\bar{1}$	43.40	44		
			∠00$\bar{4}$/01$\bar{1}$	68.30	67		
			∠00$\bar{4}$/0$\bar{1}\bar{3}$	39.95	38		

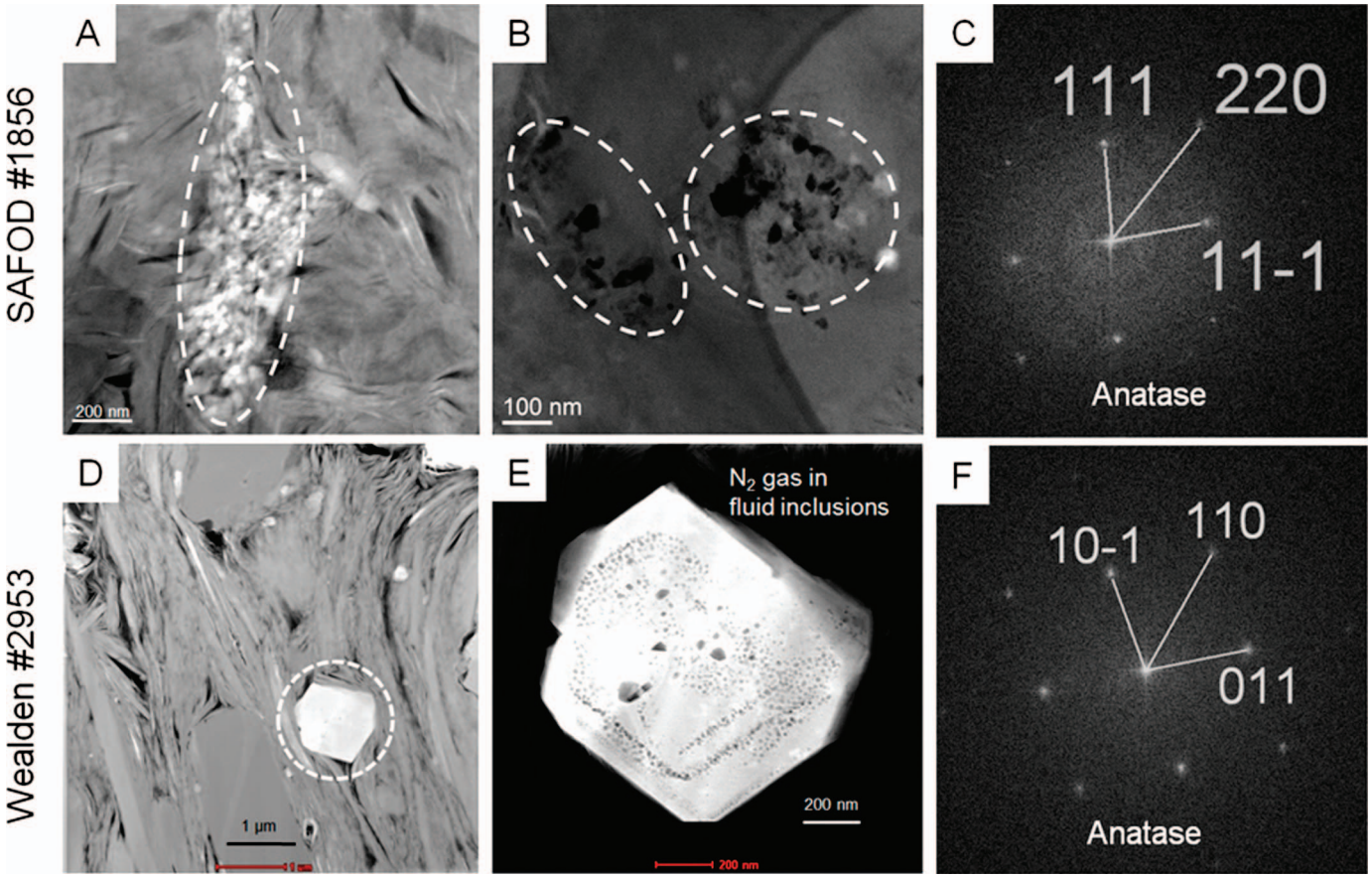

FIG. 5.—SAFOD sample #1856 (see Tables 1, 2, and 4 for sample characteristics). **A)** High-magnification scanning transmission electron microscopy (STEM) image (high-angle annular dark-field (HAADF) mode) showing a large agglomerate of anatase nano-crystals (dotted circle). **B)** High-magnification scanning transmission electron microscopy (STEM) image (high-angle annular dark-field (HAADF) mode) showing anatase agglomerates (dotted circles). **C)** FFT diffraction pattern of the anatase crystals. Zone axis is [-110]. Wealden Shale sample #2953 (see Tables 1, 2, and 4 for sample characteristics). **D)** High-magnification scanning transmission electron microscopy (STEM) image (high-angle annular dark-field (HAADF) mode) showing a large anatase crystal (dotted circle). **E)** High-magnification scanning transmission electron microscopy (STEM) image (high-angle annular dark-field (HAADF) mode) highlighting zonal fluid inclusions in the anatase crystal (filled by nitrogen gas). **F)** Electron-diffraction image of the large crystal shown in Part A proving that anatase is the titania polymorph. Zone axis is [1-11].

→

Fig. 6.—BSE images of a reservoir sandstone sample from an oil–water contact (see Table 1, 2, and 4 for sample characteristics) showing beginning rutile corrosion coupled to anatase formation. **A)** Rutile with corrosion features, **B)** pore-filling anatase cement, **C)** TEM Bright Field image of anatase agglomerate, **D)** high-magnification scanning transmission electron microscopy (STEM) image (high-angle annular dark-field (HAADF) mode) showing anatase agglomerate as in Part C, **E)** high-magnification scanning transmission electron microscopy (STEM) image (high-angle annular dark-field (HAADF) mode) showing anatase single crystals, **F)** FFT electron diffraction pattern of single anatase crystal shown in Part E. Zone-axis in 6f is [100].

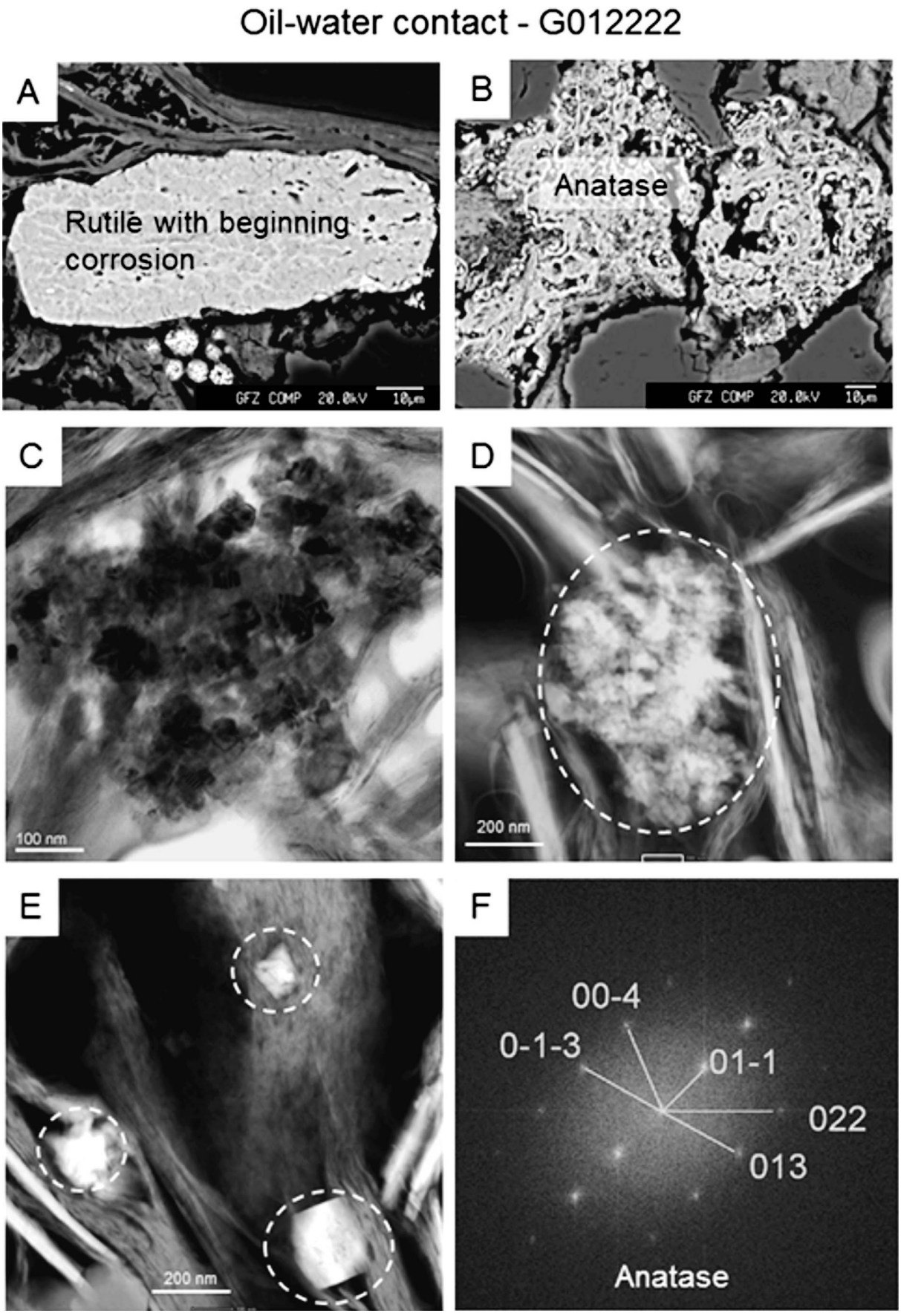
Oil-water contact - G012222
A
Rutile with beginning corrosion
GFZ COMP 20.0kV 10µm
B
Anatase
GFZ COMP 20.0kV 10µm
C
100 nm
D
200 nm
E
200 nm
F
00-4
0-1-3
01-1
022
013
Anatase

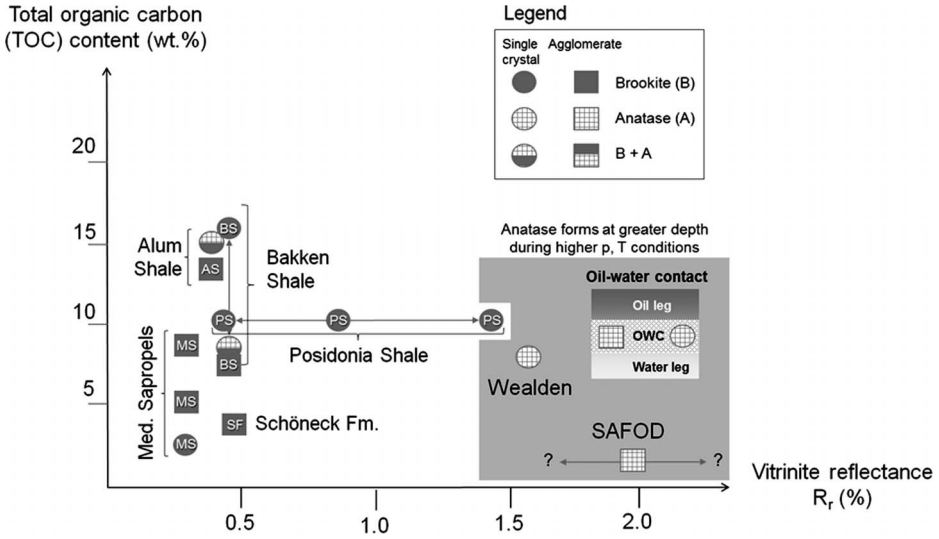

FIG. 7.—Brookite and anatase occurrence either as single crystals or as an agglomerate in relationship to TOC content and thermal maturity in the investigated samples. The gray field indicates the non-black-shale samples. In this gray field, as it does not fit into the TOC/R_r plot, the anatase occurrence at the oil–water contact in the Siri oilfield is presented as single crystals or as agglomerates.

Methodology

Polished thin sections were used to prepare electron transparent TEM foils. Prior to foil preparation, meaningful areas for investigation were selected in the sections. TEM foils were prepared using the focused-ion-beam (FIB) technique (Wirth 2004, 2009) and have the dimensions 15 µm × 10 µm × 0.150 µm.

TEM was performed in a Tecnai F20 X-Twin transmission electron microscope with an acceleration voltage of 200 kV. A Schottky field emitter was used as an electron source. The TEM is equipped with a Gatan Tridium energy filter, a Fishione high-angle annular dark-field detector (HAADF), and an EDAX X-Ray analyzer withan ultrathin window. TiO_2 nanoparticles were identified by chemical composition (EDS spectra) and from diffraction data. High-resolution lattice fringe images in low-indexed zone-axis orientation were processed applying a fast Fourier transform (FFT) to calculate a diffraction pattern. The lengths of the different vectors measured from the diffraction pattern were compared with calculated *hkl* spacing of brookite, anatase, and rutile. Additionally, the measured angles between adjacent planes were compared with the calculated angles. In those cases where the observed *d* spacing and the adjacent angles between the lattice planes are in good agreement with calculated data of the respective structure, an unambiguous identification of the TiO_2 polymorph is possible. A good agreement between the observed and calculated angles between adjacent planes is given if the deviation is less than 2°.

RESULTS

All investigated samples are rich in TOC, which ranges from 1.5% (Mediterranean Sapropel S1) to 16.4% (Bakken Shale; Table 2). The sample set covers a wide range of thermal maturity of the organic material: from immature samples such as the Mediterranean sapropels to highly mature samples such as the Wealden black shale (R_r: 1.6%; Table 2).

In TOC-rich muds from shallow sediment depth such as the Mediterranean sapropel samples of Quaternary age, brookite nanocrystals form shortly after deposition and during earliest diagenesis (Fig. 1, Table 3). After dissolution of detrital Ti-bearing minerals, diffusion as Ti^{4+}_{aq} species, and precipitation in isolated pore water cavities, these nanocrystals retain their stability during ongoing diagenesis, and remain small in size even if they agglomerate (Fig. 1H). However, continuing brookite growth during diagenesis was found in the investigated sample set of the Posidonia Shale, in which brookite crystal diameters increase from 37 nm (R_r: 0.48%) to 80 nm (R_r: 0.88%) and finally to 150–180 nm at 1.48% R_r (Fig. 2B, E, H). During increasing maturity of the Posidonia Shale, the growth of the brookite nano-crystals is coupled to a slight decrease of the oxygen indices (OI) whereas the hydrogen indices (HI) strongly decrease from 617 to 83 mgHC/gTOC (Tab. 2). The decrease of the HI values indicates a loss of potential to generate hydrocarbons. However, agglomeration has not been observed in these samples (see also Table 3). This fate and behavior of early formed brookite indicates the stability of these nanocrystals, but also favorable aqueous micro-environments capable of ongoing $Ti^{4+}_{(aq)}$ species generation and brookite precipitation.

Still immature, but at the transition to oil generation, are the samples from the Alum Shale and the Bakken Shale. Their high HI values (221 to 518 mgHC/gTOC) and low OI values (2 to 27 mgCO_2/gTOC) point to marine organic matter which is still immature (Tmax: 413–427 °C). Nearly exclusively brookite (only in one case anatase) with crystal diameters of 150–220 nm (Fig. 3H) has been detected in the Bakken Shale, partly in agglomerated form with single-crystal diameters of less than 20 nm (Fig. 3B, Table 3). In contrast, both brookite and anatase randomly occur in the Furongian to early Ordovician Alum Shale from southern Sweden (Fig. 4). Obviously, anatase occurs as idiomorphic single crystals (Fig. 4B, H), whereas brookite agglomerates are composed of single crystals with diameters of 50–100 nm (Fig. 4E). This difference in the titania polymorph type can be explained by the sedimentation rate which was extremely low for the Alum Shale (Schulz et al. 2015), and which kept anatase stable against transformation into brookite. Hence, if transformed to brookite, agglomeration took place.

Special environments where exclusively anatase forms are faults with hydrocarbon-bearing fluid flow and oil–water contacts. The peculiar growth of large anatase crystals (ca. 1.2 µm in diameter) in the Wealden sediments and the included nitrogen gas in inclusions (Fig. 5D, E; Table 4) can be explained by the special formation environment. Ahmad et al. (2012) found that anatase nanocrystals from sol–gel experiments preferentially adsorb gaseous nitrogen due to the acid character of anatase surfaces. In contrast, anatase agglomerates prevail at the SAFOD fault (Fig. 5A, B; Table 4). These agglomerates are composed of single anatase crystals less than 40 nm in size.

Oil–water contacts represent reactive interfaces in petroleum reservoirs where low molecular-weight hydrocarbons from the overlying oil leg are being dissolved and converted, via anaerobic hydrocarbon degradation, into methane, carbon dioxide, acetic acid and molecular hydrogen (see review of such processes in van Berk et al. 2013). Such processes cause low pH of the aqueous phase which is rich in dissolved organic compounds, and thus represent suitable environments for dissolution of Ti-bearing minerals such as rutile (Fig. 6A, B). Exclusively anatase has been found in such an environment of the Siri oilfield either as single crystals or as agglomerates (Table 4). Single anatase crystals can have diameters of around 200 nm (Fig. 6E) whereas the individual

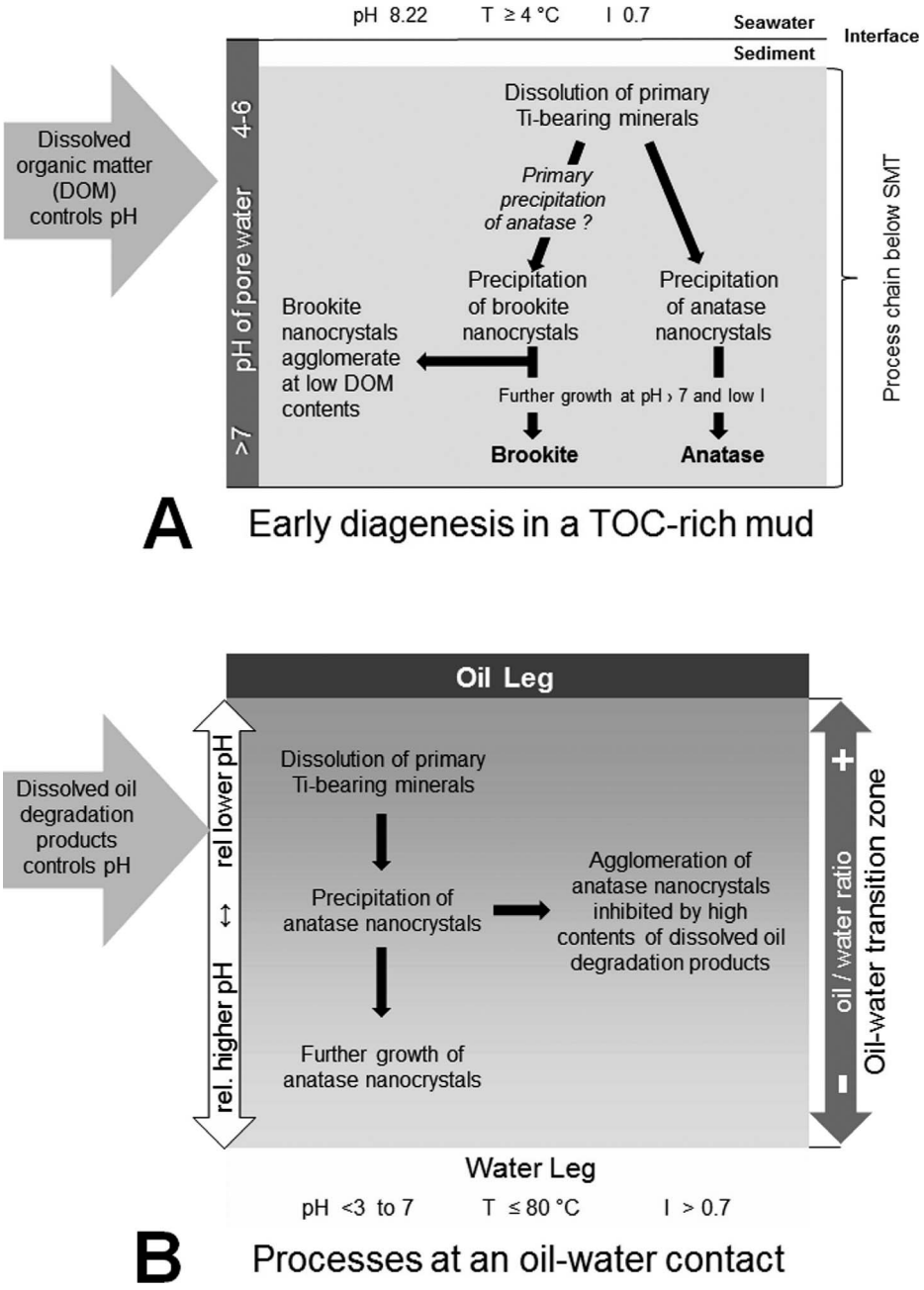

FIG. 8.—Summarizing sketches about brookite and anatase formation in black shale (Part A) and at oil–water contacts (Part B). **A)** During the methanogenic stage of early diagenesis labile organic matter is converted. Soluble organic compounds like low-molecular-weight organic acids (e.g., acetic acid, oxalic acid, etc.) lower the pH of the pore water, which leads to the dissolution of Ti-bearing detrital minerals and precipitation of brookite nanocrystals, subordinately of anatase (probably controlled by low sedimentation rate). A first precipitation of anatase as precursor of brookite is possible according thermodynamic considerations (see text and Fig. 9). If the pore water has low contents of dissolved organic matter (such as humic acids), then the brookite nanocrystals may agglomerate. Both brookite and anatase nanocrystals may continue to grow if pH of the pore water increases and ionic strength decreases. **B)** Similar processes take place at oil–water contacts in oil fields. At reservoir temperatures < 80 °C soluble oil compounds are being converted into, e.g., acetic acid, naphtenic acid, carbon dioxide, methane, etc. Their dissolution modifies the pH of the pore water which leads to the dissolution of detrital Ti-bearing minerals. Exclusively anatase nanocrystals form and continue to grow when the pH decreases. The agglomeration of anatase nanocrystals is inhibited due to the high concentration of dissolved organic compounds. Abbreviations: SMT, sulfate–methane transition zone; I, ionic strength; T, temperature.

crystals of the agglomerates are less than 50 nm in diameter (Fig. 6C). The agglomerates are similar in diameter to those found at the SAFOD fault.

In summary, brookite is the predominant titania polymorph in the investigated black shale samples, either as single crystals or as agglomerates, and the occurrence is independent on TOC content (2–16%) and thermal maturity (~ 0.3–1.6% R_r). In contrast, exclusively anatase occurs as single crystals or as agglomerates in the samples from oil–water contacts and faults (Fig. 7).

INTERPRETATIONS

The results indicate that precipitation of brookite and anatase requires specific hydrogeochemical conditions which are already established during early diagenesis in TOC-rich muds (Fig. 8A). Low pore-water pH, e.g., caused by the release of diagenetic acids such as acetic acid or oxalic acid from the organic material leads to a sufficient supply of dissolved $Ti^{4+}_{(aq)}$ species from dissolution of titanium-bearing minerals. Such acids which may control dissolution of Ti-bearing primary minerals (e.g., ilmenite, rutile, titanite, etc.) are also applied in sol–gel experiments to keep pH low.

Many of the described nanocrystals occur as individual grains, but aggregates mainly composed of brookite nanocrystals have also been found. Aggregation of firstly formed smaller crystals is reported from hydrogeochemical conditions with low contents of dissolved organic compounds whereas aggregation in natural waters is prevented by NOM (naturally occurring organic matter). The results allow no systematic interpretation on how aggregation is controlled in the investigated sample material. Moreover, also high concentrations of total dissolved solids (TDS) favor aggregation.

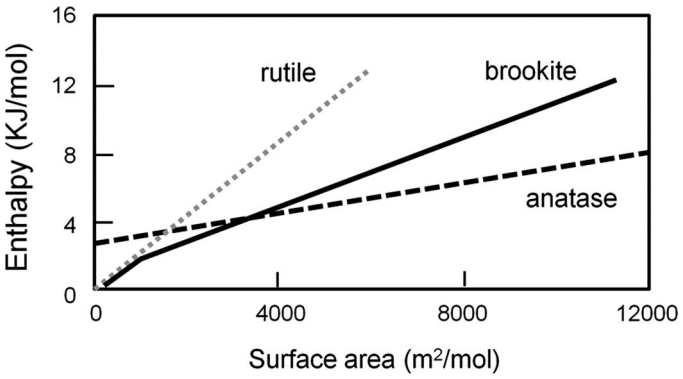

FIG. 9.—Enthalpy of titania polymorphs as a function of surface area (redrawn after Navrotsky 2004, basically after Ranade et al. 2002). Although the crystalline polymorph rutile is thermodynamically the most stable one, anatase and brookite are often only slightly metastable by only a few kilojoules per mole. Brookite has a surface enthalpy of approximately 1.0 J/m^2, which is higher than for anatase (0.4 J/m^2). Moreover, for titania particles with a surface area higher than around 4,000 m^2/mol (thus for smallest particles), anatase has the lowest enthalpy and can directly transform into brookite (Ranade et al. 2002). At a crossover size of about 30 nm anatase nanoparticles may directly transform into rutile (Zhang and Banfield 1998; Navrotsky 2003).

It is obvious that especially brookite nanocrystal growth is contingent upon low pH and low temperatures of the aqueous phase in which reactions take place. As most of the samples are from marine depositional environments, the formation water during early diagenesis is still high in total dissolved solids as it is originally seawater. Coupled to low pH, aggregation of nanocrystals with similar size takes place. However, similar aggregates composed of anatase nanocrystals have not been found in the investigated black shale samples (Fig. 8A).

Conditions of acidic pore water would be buffered in the presence of carbonate such as calcite, which occurs in all investigated Posidonia Shale samples. As a consequence, dissolution and precipitation of titania would thus not be possible. However, brookite and anatase occur in two different environments in shale, either in open pore space (e.g., reservoir sandstone in Fig. 6) or in black shales predominantly in "closed" micro-environments, e.g., in clay minerals or mica. However, acidic and corrosive pore-water characteristics may develop in both environments. According to this, micro-environments similar to those in black shales may develop in carbonate-bearing sediments and may enable localized titania precipitation.

Moreover, precipitation of brookite or anatase nanocrystals is not limited to black shale environments. The hydrogeochemical properties of the aqueous phase are the actual control on brookite and anatase nanocrystal formation, and titania may form in all other environments with similar characteristics. The main hydrogeochemical parameter which determines titania formation is low pH and is controlled by acid release during early diagenesis of TOC-rich mud or in soil profiles, but also by oil degradation at OWCs or in the oil leg (Fig. 8B). In general, nucleating anatase grains are characterized by lower enthalpy (< 8 kJ/mol) compared to brookite (>10 kJ/mol; Fig. 9). During growth, the decrease of enthalpy is lower for anatase than for brookite, and at surface areas of around 4,000 m^2/mol brookite is lower in enthalpy. According to this, first formed nuclei should be tetragonal anatase which becomes unstable during growth in comparison to the orthorhombic brookite structure. Rapid crystallization, on the one hand, would thus favor the nucleation and persistence of anatase. Slow growth, on the other hand, would enable transformations into metastable brookite, which would finally transform into the stable rutile polymorph (Benning and Waychunas 2008). As organic-rich mud undergoes rapid geochemical changes shortly after deposition (from oxic pore-water conditions to sulfate reduction to methanogenesis), the anatase-preserving conditions may change rapidly and may lead to transformation into brookite (Fig. 8A) whereas similar pore-water conditions at greater depth may become established over longer periods, leading to conditions suitable for anatase stability and growth (Fig. 8B). Such stable pore-water conditions may also explain the occurrence of predominantly anatase in the Alum Shale (Fig. 4B, H), which was deposited over a time span of 20 My under similar conditions.

Density-functional-theory calculations performed by Li et al. (2008) showed that brookite surfaces may adsorb higher contents of formic acid, in contrast to anatase. Dissolved formic acid is, besides dissolved acetic acid and oxalic acid, one of the major low-molecular-weight organic acids (LMWOAs) which are generated during earliest diagenesis at shallow sediment depth (e.g., Xiao et al. 2009, 2010). However, adsorption of LMWOAs on titania nanoparticles is controlled by pH of aqueous solutions. Humic acids, e.g., are preferentially adsorbed at pH lower than 5, whereas adsorption decreases at pH higher than 5. In conclusion, brookite crystallization during early diagenesis is controlled by low pH when organic acids are preferentially adsorbed.

Brookite predominates over anatase in the investigated black shales (Fig. 7). Brookite was found either as single crystals (mainly as platy crystals, partly with thickness fringes due to diffraction contrasts) or as aggregates. In general, a high ionic strength of an aqueous solution promotes titania nanocrystal aggregation (Domingos et al. 2009; French et al. 2009). Samples with brookite aggregates occur in marine environments (Mediterranean sapropels, Bakken Shale, and Alum Shale), and high ionic strength of the sediment pore water can be assumed (Fig. 8A). In contrast, agglomeration was not observed in the Posidonia Shale, which is also marine in origin. The reasons why the hydrogeochemical characteristics of pore water in the Posidonia Shale during early diagenesis, but also later, did not lead to agglomerates are difficult to evaluate. It is the complex interplay of multiple factors such as ionic strength, pH and resulting acid adsorption which controlled whether nanocrystals agglomerate or not.

CONCLUSIONS

Brookite and anatase nano-crystals form in hydrogeochemical environments at low pH, with mainly brookite at sediment temperatures of less than 10°C during early diagenesis. The preferred precipitation of brookite is dependent on the release of diagenetic products such as CO_2, CH_4, H_2, LMWOAs or the early diagenetic formation of humic and fulvic acids. Besides these formation controls, results from other studies indicate that the ionic strength of the aqueous solution may also modify the agglomeration tendency (e.g., Chen et al. 2012). Such conditions are strongly coupled with available soluble organic matter, and occur in black shales with TOC values over a wide range (1.5 to 16.4 wt.% TOC). After the initial precipitation of brookite nano-crystals, their growth may continue during further burial provided that the hydrogeochemical conditions remain stable.

In other TOC-rich environments with higher thermal maturities and high present-day temperatures (more than 60°C) according to the prevailing burial depth, exclusively anatase forms independently of lithology such as in sandstone reservoirs in oilfields or in permeable zones in shale with fluid flow. The predominance of anatase along faults and at oil–water contacts at higher temperatures additionally reflects stable hydrogeochemical conditions in contrast to changing conditions during early diagenesis.

The formation of predominantly brookite in black shale is furthermore dependent on isolated micro-environments in which acidic and corrosive conditions may lead to dissolution of titanium-bearing minerals. Dissolved $Ti^{(4+)}_{aq}$ species in pore waters as a source for the observed titania precipitations can be due to the occurrence of detrital rutile, ilmenite, titanite, etc. Such micro-environments can exclusively develop in isolated, water-wet cavities of impermeable TOC-rich clayey sediments during early diagenesis.

ACKNOWLEDGMENTS

We would like to acknowledge a number of colleagues who contributed to this study through providing material for investigations. These include Jürgen Möbius (Hamburg, Germany), Rolando di Primio (Oslo, Norway), Johan Byskov Svendsen and Niels. H. Schovsbo (both Copenhagen, Denmark), and Christoph Janssen

(Potsdam, Germany). The final paper profited greatly from very thorough and helpful reviews by Georgia Pe-Piper and an anonymous reviewer. We also thank JSR editor Leslie Melim and associate editor Sally Sutton, and technical editor John Southard for providing helpful comments and for editorial handling of this manuscript.

REFERENCES

Ahmad, M.A., Prelot, B., Razafitianamaharavo, A., Douillard, J.M., Zajac, J., Dufour, F., Durupthy, O., Chaneac, C., and Villiéras, F., 2012, Influence of morphology and crystallinity on surface reactivity of nanosized anatase TiO_2 studied by adsorption techniques. 1. The Use of Gaseous Molecular Probes: The Journal of Physical Chemistry C, v. 116, p. 24,596-24,606.

Banfield, J.F., Bischoff, B.L., and Anderson, M.A., 1993, TiO_2 accessory minerals: coarsening, and transformation kinetics in pure and doped synthetic nanocrystalline materials: Chemical Geology, v. 110, p. 211–231.

Benning, L.G., and Waychunas, G.A., 2008, Nucleation, growth, and aggregation of mineral phases: mechanisms and kinetic controls, *in* Brantley, S.L., Kubicki, J.D., and White, A.F., eds., Kinetics of Water–Rock Interaction: New York, Springer, p. 259–333.

Bernard, S., Horsfield, B., Schulz, H.-M., Schreiber, A., Wirth, R., Vu, T.T.A., Perssen, F., Könitzer, S., Volk, H., and Sherwood N., 2012, Multi-scale detection of organic and inorganic signatures provides insights into gas shale properties and evolution: Chemie der Erde, Geochemistry, v. 70, p. 119–133.

Bhave, R.C., and Lee, B.I., 2007, Experimental variables in the synthesis of brookite phase TiO_2 nanoparticles: Materials Science and Engineering, v. A 467, p. 146–149.

Brookins, D.G., 1988, Eh–pH Diagrams for Geochemistry: New York, Springer-Verlag, 176 p.

Cabral, A.R., Reith, F., Lehmann, B., Brugger, J., Meinhold, M., Tupinambá, M., and Kwitko-Ribeiro R., 2012, Anatase nanoparticles on supergene platinum–palladium aggregates from Brazil: titanium mobility in natural waters: Chemical Geology, v. 334, p. 182–188.

Chen, G., Liu, X., and Su, C., 2012, Distinct effects of humic acid on transport and retention of TiO_2 rutile nanoparticles in saturated sand columns: Environmental Science and Technology, v. 46, p. 7142-7150.

Collins, G., 1975, Geochemistry of oilfield waters: Amsterdam, Elsevier, Developments in Petroleum Science, v. 1, 495 p.

Cornu, S., Lucas, Y., Lebon, E., Ambrosi, J.P., Luizáo, F., Rouiller, J., Bonnay, M., and Neal, C., 1999, Evidence of titanium mobility in soil profiles, Manaus, central Amazonia: Geoderma, v. 91, p. 281–295.

Deng, Y., and Dixon, J.B., 2002, Soil organic matter and organic–mineral interactions, *in* Soil Science Society of America, ed., Soil Mineralogy with Environmental Application: Soil Science Society of America, Book Series 7, p. 69–107.

Domingos, R.F., Tufenkji, N., and Wilkinson, K.J., 2009, Aggregation of titanium dioxide nanoparticles: role of a fulvic acid: Environmental Science and Technology, v. 43, p. 1282–1286.

Dumon, J.C., and Vigneaux, M., 1979, Evidence for some mobility of titanium in podzols and under laboratory conditions as a result of the action of organic agents: Physics and Chemistry of the Earth, v. 11, p. 331–337.

Erzinger, J., Wiersberg, T., and Zimmer, M., 2006, Real-time mud gas logging and sampling during drilling: Geofluids, v. 6, p. 225–233.

Fang, J., Shan, X., Wen, B., Lin, J., and Owens, G., 2009, Stability of titania nanoparticles in soil suspensions and transport in saturated homogeneous soil columns: Environmental Pollution, v. 157, p. 1101–1109.

Finnegan, M.P., Zhang, H., and Banfield, J.F., 2007, Phase stability and transformation in titania nanoparticles in aqueous solutions dominated by surface energy: The Journal of Physical Chemistry, v. C 111, p. 1962–1968.

Fitzpatrick, R.W., Le Roux, J., and Schwetmann, U., 1978, Amorphous and crystalline titanium and iron-titanium oxides in synthetic preparations, at near ambient conditions, and in soil clays: Clays and Clay Minerals, v. 26, p. 189–201.

Fitzpatrick, R.W., and Chittleborough, D.J., 2002, Titanium and zirconium minerals, in Soil Science Society of America, ed., Soil Mineralogy with Environmental Applications: Soil Science Society of America, Book Series 7, p. 667–690.

French, R.A., Jacobson, A.R., Kim, B., Isley, S.L., Penn, R.L., and Baveye, P.C., 2009, Influence of ionic strength, pH, and cation valence on aggregation kinetics of titanium dioxide nanoparticles: Environmental Science and Technology, v. 43, p. 1354–1359.

Hays, P.D., James, W.D., and Tieh, T.T., 1994, The role of NAA in studies of organic diagenesis of rocks: Journal of Radioanalytical and Nuclear Chemistry, v. 180, p. 15–23.

Helgeson, H.C., Knox, A.M., Owens, C.E., and Shock, E.L., 1993, Petroleum, oil field waters, and authigenic mineral assemblages: Are they in metastable equilibrium in hydrocarbon reservoirs?: Geochimica et Cosmochimica Acta, v. 57, p. 3295–3339.

Huberty, J., and Xu, H., 2008, Kinetics study on phase transformation from titania polymorph brookite to rutile: Journal of Solid State Chemistry, v. 181, p. 508–514.

Isley, S.L., and Penn, L.R., 2006, Relative brookite and anatase content in sol–gel-synthesized titanium dioxide nanoparticles: Journal of Physical Chemistry B, v. 110, p. 15134–15139.

Isley, S.L., and Penn, L.R., 2008, Titanium Dioxide Nanoparticles: effect of sol-gel pH on phase composition, particle size, and particle growth mechanism: Journal of Physical Chemistry C, v. 112, p. 4469–4474.

Isley, S.L., Anderson, E.R., and Penn, R.L., 2006, Influence of ionic strength on brookite content in sol–gel synthesized titania before and after hydrothermal aging: Electrochemical Society, Transactions, v. 3, p. 37–46.

Isley, S.L., Jordan, D.S., and Penn, L.R., 2009, Titanium dioxide nanoparticles: impact of increasing ionic strength during synthesis, reflux, and hydrothermal aging: Materials Research Bulletin, v. 44, p. 119–125.

Janssen, C., Wirth, R., Wenk, H.-R., Morales, L., Naumann, R., Kienast, M., and Dresen, G., 2014, Faulting processes in active faults: evidence from TCDP and SAFOD drill core samples: Journal of Structural Geology, v. 65, p. 100–116.

Keller, A.A., Wang, H., Zhou, D., Lenihan, H.S., Cherr, G., Cardinale, B.J., Miller, R., and Ji, Z., 2010, Stability and aggregation of metal oxide nanoparticles in natural aqueous matrices: Environmental Science and Technology, v. 44 , p. 1962–1967.

Kuhn, P., R., Di Primio, and Horsfield, B., 2010, Bulk composition and phase behaviour of petroleum sourced by the Bakken Formation of the Williston Basin: Geological Society of London, Petroleum Geology Conference series, v. 7, p. 1065–1077.

Li, W.-K., Gong, X.-Q., Lu, G., and Selloni, A., 2008, Different reactivities of TiO_2 polymorphs: comparative DFT calculations of water and formic acid adsorption at anatase and brookite TiO_2 surfaces: Journal of Physical Chemistry, v. C 112, p. 6594–6596.

Lockner, D.A., Morrow, C., Moore, D., and Hickman, S., 2011, Low strength of deep San Andreas fault gouge from SAFOD core: Nature, v. 472, p. 82–85.

Malengreau, N., Muller, J.P., and Calas, G., 1995, Spectroscopic approach for investigating the status and mobility of Ti in kaolinitic materials: Clays and Clay Minerals, v. 43, p. 615–621.

Morad, S., 1986, Pyrite–chlorite and pyrite–biotite relations in sandstones: Sedimentary Geology, v. 49, p. 177–192.

Morad, S., and Aldahan, A.A., 1986, Alteration of detrital Fe-Ti oxides in sedimentary rocks: Geological Society of America, Bulletin, v. 97, p. 567–578.

Morad, S., and Aldahan, A.A., 1987a, Diagenetic replacement of feldspars by titanium oxides in sandstones: Sedimentary Geology, v. 51, p. 147–153.

Morad, S., and Aldahan, A.A., 1987b, Diagenetic chloritization of feldspars in sandstones: Sedimentary Geology, v. 51, p. 155–164.

Mu, N., Schulz, H.-M., Fu, Y., Wirth, R., Rhede, D., and van Berk, W., 2015, Berthierine formation in an oil reservoir as result of fluid–rock interactions: Part I. Characterization: Marine and Petroleum Geology, v. 65, p. 302–316.

Navrotsky, A., 2004, Energetic clues to pathways to biomineralization: precursors, clusters, and nanoparticles: National Academy of Science (USA), Proceedings, v. 101, p. 12,096–12,101.

Neale, P.A., Jämting, Å.K., O'Malley, E., Herrmann, J., and Escher, B.I., 2015, Behaviour of titanium dioxide and zinc oxide nanoparticles in the presence of wastewater-derived organic matter and implications for algal toxicity: Environmental Science: Nano, v. 2, p. 86–93.

Parnell, J., 2004, Titanium mobilization by hydrocarbon fluids related to sill intrusion in a sedimentary sequence, Scotland: Ore Geology Reviews, v. 24, p. 155–167.

Pe-Piper, G., Karim, A., and Piper, D.J.W., 2011, Authigenesis of titania minerals and the mobility of Ti: new evidence from pro-deltaic sandstones, Cretaceous Scotian Basin, Canada: Journal of Sedimentary Research, v. 81, p. 762–773.

Pettibone, J.M., Cwiertny, D.M., Scherer, M., and Grassian, V.H., 2008, Adsorption of organic acids on TiO_2 nanoparticles: effects of pH, nanoparticle size, and nanoparticle aggregation: Langmuir, v. 24, p. 6659–6667.

Post, J.E., and Burnham, C.W., 1986, Ionic modeling of mineral structures and energies in the electron gas approximation: TiO_2 polymorphs, quartz, forsterite, diopside: American Mineralogist, v. 71, p. 1142–1150.

Ranade, M.R., Navrotsky, A., Zhang, H.Z., Banfield, J.F., Elder, S.H., Zaban, A., Borse, P. H., Kulkarni, S.K., Doran, G.S., and Whitfield, H.J., 2002, Energetics of nanocrystalline TiO_2: National Academy of Science (USA), Proceedings, v. 99, suppl. 2, p. 6476–6481.

Schroeder, P.A., and Shiflet, J., 2000, Ti-bearing phases in the Huber Formation, an East Georgia kaolin deposit: Clays and Clay Minerals, v. 48, p. 151–158.

Schulz, H.-M., Sachsenhofer, R.F., Bechtel, A., Polesny, H., and Wagner, L., 2002, The origin of hydrocarbon source rocks in the Austrian Molasse Basin (Eocene–Oligocene transition): Marine and Petroleum Geology, v. 19, p. 683–709.

Schulz, H.-M., Biermann, S., van Berk, W., Krüger, M., Straaten, N., Bechtel, A., Wirth, R., Lüders, V., Schovsbo, N.H., and Crabtree, S., 2015, From shale oil to biogenic shale gas: retracing organic–inorganic interactions in the Alum Shale (Furongian–Lower Ordovician) in southern Sweden: American Association of Petroleum Geologists, Bulletin, v. 99, p. 927–956.

Seewald, J.S., 2003, Organic–inorganic interactions in petroleum-producing sedimentary basins: Nature, v. 426, p. 327–333.

Skrabal, S.A., 1995, Distributions of dissolved titanium in Chesapeake Bay and the Amazon River Estuary: Geochimica et Cosmochimica Acta, v. 59, p. 2449–2458.

Swaine, D.J., and Mitchell, R.L., 1960, Trace-element distribution in soil profiles: Journal of Soil Science, v. 11, p. 347–368.

Tuschel, D., 2013, Raman spectroscopy of oil shale: Spectroscopy, v. 28, 5 p.

van Berk, W., Schulz, H.-M., and Fu, Y., 2013, Controls on CO_2 fate and behavior in the Gullfaks oilfield (Norway): how hydrogeochemical modeling can help to decipher organic–inorganic interactions: American Association of Petroleum Geologists, Bulletin, v. 97, p. 253–262.

Wirth, R., 2004, A novel technology for advanced application of micro- and nanoanalysis in geosciences and applied mineralogy: European Journal of Mineralogy, v. 16, p. 863–876.

Wirth, R., 2009, Focused Ion Beam (FIB) combined with SEM and TEM: advanced analytical tools for studies of chemical composition, microstructure and crystal structure in geomaterials on a nanometre scale: Chemical Geology, v. 261, p. 217–229.

Xiao, M., Wu, F., Liao, H., Li, W., Lee, X., and Huang, R., 2009, Vertical profiles of low molecular weight organic acids in sediment porewaters of six Chinese lakes: Journal of Hydrology, v. 365, p. 37–45.

Xiao, M., Wu, F., Liao, H., Li, W., Lee, X., and Huang, R., 2010, Characteristics and distribution of low molecular weight organic acids in the sediment porewaters in Bosten Lake, China: Journal of Environmental Sciences, v. 22, p. 328–337.

Yang, K., Lin, D., and Xing, B., 2009, Interactions of humic acid with nanosized inorganic oxides: Langmuir, v. 25, p. 3571–3576.

Zhang, H., and Banfield, J.F., 1998, Thermodynamic analysis of phase stability of nanocrystalline titania: Journal of Materials Chemistry, v. 8, p. 2073–2076.

Received 2 February 2015; accepted 17 October 2015.